微生物学报
Acta Microbiologica Sinica
2018, 58(12): 2186-2203
http://journals.im.ac.cn/actamicrocn
DOI: 10.13343/j.cnki.wsxb.20180045

Research Article 研究报告

Mechanisms of MSMEG_3312-mediated collective antibiotic tolerance to erythromycin in mycobacteria revealed by quantitative proteomic analysis

Yujiao Zhang[1,2#], Xinling Hu[1#], Xiaojing Li[1], Haiteng Deng[3*], Kaixia Mi[1,4*]

[1] CAS Key Laboratory of Pathogenic Microbiology and Immunology, Institute of Microbiology, Chinese Academy of Science, Beijing 100101, China
[2] College of Life Sciences, University of Chinese Academy of Sciences, Beijing 101408, China
[3] School of Life Sciences, Tsinghua University, Beijing 100084, China
[4] Savaid Medical School, University of Chinese Academy of Sciences, Beijing 101408, China

Abstract: [Objective] The effects of antibiotics on bacteria are complex, and bacterial response to antibiotics is just beginning to be understood using systems biology. We previously showed that a hemerythrin-like protein, MSMEG_3312, is involved in erythromycin susceptibility. In this study, we explore the mechanisms of collective antibiotic tolerance to erythromycin in mycobacteria through the hemerythrin-like protein MSMEG_3312. **[Methods]** We analyzed MSMEG_3312 secondary structure using spectrophotometric and circular dichroism (CD) methods. Tandem mass tag(TMT)-labeled quantitative proteomics was used to compare protein level changes between the wild type strain mc^{2}155 and the knockout strain *Δmsmeg_3312*, following bioinformatics analysis. Differentially expressed proteins were also verified by qPCR. To confirm our analyses' conclusions that transporters are involved in MSMEG_3312-related erythromycin susceptibility, we also measured the concentration of mycobacterial erythromycin *in vivo* in the wild type strain mc^{2}155 and *Δmsmeg*_3312 using an erythromycin ELISA kit. **[Results]** Initially, we confirmed that MSMEG_3312 is a redox-related hemerythrin-like protein using spectrophotometric and CD analysis. Quantitative proteomic analysis revealed that *Δmsmeg_3312* has eight up-regulated proteins, including three transporters, and 14 down-regulated proteins, compared with the wild type strain mc^{2}155, while growing in 7H9 medium. In contrast, 448 proteins were identified as being differentially expressed between mc^{2}155 and *Δmsmeg_3312*, when treated with erythromycin, of which 11 were identified as up-regulated transporter proteins, and 26 were associated with amino acid synthetic pathways. The intracellular erythromycin concentration in *Δmsmeg_3312* was also lower than in mc^{2}155. **[Conclusion]** We show that MSMEG_3312 mediates erythromycin resistance due to collective antibiotic tolerance arising from antibiotic

Supported by the Ministry of Science and Technology of China (2017YFA0505901, 2014CB744402) and by the National Natural Science Foundation of China (NSFC) (31670137 to K.M., 31600114 to H.X., 31700128 to L.X.)

*Corresponding authors. Kaixia Mi, Tel: +86-10-64806082, Fax: +86-10-64807468, E-mail: mik@im.ac.cn; Haiteng Deng, Tel: +86-10-62790498, Fax: +86-10-62797154, E-mail: dengh@biomed.tsinghua.edu.cn
#These authors contributed equally to this work.

Received: 26 January 2018; Revised: 30 March 2018; Published online: 28 May 2018

titration and high-density populations.

Keywords: quantitative proteomics, hemerythrin-like protein, MSMEG_3312, mycobacteria, erythromycin, collective antibiotic tolerance

Antibiotics have saved more than millions of lives, but currently the prevalence of antibiotic-resistant pathogens is a global threat. However, antibiotic effects on bacteria are complex, and bacterial response to antibiotic drug treatment is just beginning to be understood using biological systems approaches[1–3].

Tuberculosis (TB) remains a formidable challenge to global health and is caused by an ancient pathogen, *Mycobacterium tuberculosis*[4]. A recent study comparing genomes to examine *M. tuberculosis* complex (MTBC) evolution indicates that *M. tuberculosis* co-evolved with modern humans[5]. In the pre-antibiotic era, TB caused nearly 20% of all deaths in Europe from the seventeenth through the nineteenth centuries[6]. Millions of lives have subsequently been saved through chemotherapy by the addition of antibiotics to the TB treatment regimen. However, standard anti-tuberculosis therapy is only effective for drug-susceptible TB, not multi-drug-resistant (MDR) and extensively-drug-resistant (XDR) TB. Unfortunately, our knowledge of drug resistance in mycobacteria remains incomplete, presenting obstacles to the development of new anti-tubercular drugs[7]. The basic mechanisms of drug resistance in mycobacteria are complicated, although the techniques of systems biology are beginning to answer questions at the systems level[8], providing new insights into the outcome of drug resistance and for designing control strategies against *M. tuberculosis*.

Many studies have shown antibiotic resistance to be correlated with redox regulation[9]. For example, isoniazid (isonicotinic acid hydrazide, INH) is an important first-line anti-mycobacterial antibiotic that has been widely used in the treatment of active and latent TB[10]. INH is activated by the bacterial catalase-peroxidase KatG, which is encoded by *rv1908c*[11]. KatG-mediated INH activation produces a range of highly reactive oxygen species, including superoxide and hydroxyl radicals[12], and oxidative stress decreases isoniazid resistance in *M. tuberculosis*[10]. Recently, rifampin (RIF), a first-line anti-TB drug, was shown to induce hydroxyl radical formation in *M. tuberculosis*[13–14]. These studies suggest that redox-related proteins influence antibiotic effects in *M. tuberculosis*.

Previous studies have focused on the response of single event in response to antibiotics. However, Collective antibiotic tolerance is not a single event, but a combination of diverse mechanisms, including transporter induction, antibiotic titration, bacterial population, and biofilm formation[15–18]. Few studies have reported collective antibiotic tolerance mechanisms in mycobacterial resistance[15].

Hemerythrin-like proteins are present in all domains of life[19–20]. Several studies have shown that these proteins can function as oxygen sensors, and to store oxygen reserves, as well as to transport oxygen[20]. Hemerythrin-like proteins with oxygen-carrier capabilities might interfere with antibiotic response.

The pathogen *M. tuberculosis* and the soil microorganism *Mycobacterium smegmatis* share many genetic systems. In particular, genes that participate in sensing and responding to stress are conserved between *M. tuberculosis* and *M. smegmatis*[21]. These genes enable survival under environmental stress, including oxidative stress, hypoxia, and exposure to multiple antimicrobial agents[22–23]. *M. smegmatis* has three hemerythrin-like proteins, MSMEG_3312, MSMEG_2415 and

MSMEG_6212[24–26]. Our previous studies showed that MSMEG_2415 plays an important role in H_2O_2 susceptibility[24], while MSMEG_3312 and MSMEG_6212 modulate erythromycin susceptibility[25]. Additionally, MSMEG_3312 plays a relative dominate role in erythromycin susceptibility, compared with MSMEG_6212[25]. However, the mechanisms of MSMEG_3312 on erythromycin in mycobacteria have not yet been studied.

In this study, we used *M. smegmatis*, a *M. tuberculosis* model organism[21], to identify the mechanisms of antibiotic responses. We first characterized MSMEG_3312 as a hemerythrin-like protein, showing that it possesses a typical hemerythrin domain motif H…HxxxE…HxxxH…HxxxxD/E[20]. By combining a quantitative proteomic analysis, the intracellular concentration of erythromycin, and an erythromycin killing curve, we provide a model of collective antibiotic tolerance (CAT) to explain the role of MSMEG_3312 in mediated erythromycin resistance: Constitutively higher levels of transporters in *Δmsmeg_3312* compared with mc^{2}155 facilitates lower levels of intracellular erythromycin in *Δmsmeg_3312,* generating a positive feedback loop that overcomes erythromycin- mediated inhibition of ribosome activity and enables higher population survival. Increasing cell densities lead to an increase in total protein production, thus decreasing erythromycin titers in *Δmsmeg_3312*, which results in a more resistant phenotype, compared with mc^{2}155.

1 Materials and Methods

1.1 Culture medium and growth conditions

Liquid cultures of *M. smegmatis* strains were grown in Middlebrook 7H9 medium (Becton Dickinson, Sparks, MD, USA) supplemented with ADS enrichment [Albumin-Dextrose Saline containing 5% (*W/V*) bovine serum albumin fraction V, 2% (*W/V*) D-dextrose, 8.1% (*W/V*) NaCl, 0.5% (*V/V*) glycerol, and 0.05% (*V/V*) Tween80]. Antibiotics were used as described: Hygromycin (75 mg/L for *M. smegmatis*, 150 mg/L for *Escherichia coli*; Roche) and kanamycin (25 mg/L for *M. smegmatis*, 50 mg/L for *E. coli*; AMERCO) were added to the medium as needed. The wild type *M. smegmatis* strains mc^{2}155, *Δmsmeg_3312*, and *E. coli* strains DH5α, BL21(DE3) were stored in our lab. The drug exposure experiments were performed as we previously described[27]. Briefly, cultures were started from glycerol-frozen stocks and grown to log phase (OD_{600} of 0.6–0.8), then mycobacterial cells were diluted approximately 10^7-fold in fresh medium. After the addition of 31.25 mg/L erythromycin, aliquots were removed at the indicated times and plated on 7H10-ADS. Experiments were performed in triplicate. Standard deviations are indicated by error bars. *t*-tests were performed using online GraphPad software. ** P<0.01.

1.2 Cloning, expression and purification of MSMEG_3312 in *Escherichia coli*

The *msmeg_3312* coding sequence was amplified from *M. smegmatis* mc^{2}155 strain genomic DNA and cloned into the expression vector pET23b (+) (Novagen, USA) in-frame, producing a fusion protein with a C-terminal 6×His-tag sequence to generate the plasmid pET23b-3312, which was transformed into *E. coli* BL21(DE3) (Invitrogen, USA) for expression. Recombinant MSMEG_3312 was induced by incubation with 0.5 mmol/L isopropyl β-D-thiogalactoside (IPTG) at 28 °C for 3 h. Cells were harvested by centrifugation at 10000×g for 5 min, resuspended in lysis buffer [20 mmol/L Tris-HCl pH 8.0; 1 mol/L NaCl, 10% (*V/V*) glycerol, 20 mmol/L imidazole, 0.1% (*V/V*) Triton X-100, 1 mmol/L phenylmethylsulfonyl fluoride (PMSF), 1 mg/mL (*W/V*) lysozyme] and lysed by sonication. Lysates were centrifuged at 12000 r/min for 30 min at 4°C to remove debris before purification. The supernatants were incubated with Ni-NTA agarose (Qiagen, USA) with rotation for 4 h at 4 °C. Beads were then washed three times with washing buffer [20 mmol/L Tris-HCl pH 8.0,

0.5 mol/L NaCl, 10% (*V/V*) glycerol, 50 mmol/L imidazole, 0.1% (*V/V*) Triton X-100, 1 mmol/L PMSF, 25 mmol/L $MgCl_2$]. The proteins were eluted with elution buffer [50 mmol/L Tris-HCl pH 7.5, 0.5 mol/L NaCl, 25 mmol/L $MgCl_2$, 10% (*V/V*) glycerol, 300 mmol/L imidazole] and protein concentration was measured using the bicinchoninic acid protein assay reagent and a BSA standard. Purified protein was examined using 12% sodium dodecyl sulfate polyacrylaminde gel electrophoresis to verify molecular weight and purity.

1.3 Spectrophotometric and circular dichroism (CD) analysis of MsmHr

Purified MSMEG_3312 was diluted in 20 mmol/L Tris-HCl buffer (pH 7.5). Deoxy samples were obtained by adding a 10-fold molar excess of $Na_2S_2O_4$ to MSMEG_3312. UV-Vis spectrophotometric spectra were obtained in 1 mm path length quartz cuvettes on a 2802H UV-Vis spectrophotometer (Unico Shanghai Instruments Co., Ltd., China). Spectra of deoxy-MSMEG_3312 were collected in an anaerobic incubator (Shanghai Yuejin Medicial Instruments Co., Ltd, China). CD measurements were performed using a Chirascan Circular Dichroism Spectrometer (Applied Photophysics Ltd. UK). The analysis software provided with the instrument was used for analysis of the results.

1.4 MS sample preparation and peptide TMT-labeling

To analyze differences in protein levels between the wild type strain mc^2155 and knockout strain Δ*msmeg*_3312 with or without erythromycin, tandem mass tag(TMT)-labeled proteomic analyses were performed. Briefly, the strains were propagated in three independent 50 mL cultures in 7H9 medium. Fifty-milliliter cultures of the wild-type strain mc^2155 or *Δmsmeg_3312* strain were harvested by centrifugation when the OD_{600} of the cultures reached 0.3.

The corresponding cell pellets were washed once and resuspended in phosphate buffer saline (PBS) containing 8 mol/L urea at pH 7.2. Next protein extracts were prepared using a Mini BeadBeater (BioSpec), and the protein concentrations were examined using the bicinchoninic acid protein assay reagent, with a BSA standard. Protein extracts (200 μg) from wild type strain mc^2155 or Δ*msmeg_3312* strain were reduced with 10 mmol/L dithiothreitol (DTT) and alkylated with 55 mmol/L iodoacetamide.

Sequencing-grade modified trypsin (Promega, Fitchburg, WI, USA) was used for digestion in 50 mmol/L ammonium bicarbonate at 37 °C overnight. After digestion, the peptides were extracted with 50% acetonitrile solution supplemented with 0.1% trifluoroacetic acid for 30 min. The solution was clarified by centrifugation. The resulting peptides were then desalted using Sep-Pak® Vac 3cc (500 mg) certified tC18 Cartridges (Waters Corporation, Waters, MA, USA) followed by TMT labeling. Peptides from mc^2155 and *Δmsmeg_3312* without erythromycin treatment were labeled with TMT^6-127 and TMT^6-128, and peptides from mc^2155 and *Δmsmeg_3312* with erythromycin treatment were labeled with TMT^6-129 and TMT^6-130, respectively. Next, the desalted samples were fractionated using a 4.6 mm × 250 mm C_{18} column (Waters Corporation) on a Waters HPLC system (Waters Corporation). Buffer A consisted of water (pH 10) and buffer B consisted of 98% acetonitrile (ACN) (pH 10). 47 fractions were collected during a 70-min gradient of 5% to 95% buffer B. Solvent from each fraction was dried in a Speed Vac, then combined into 10 fractions, and stored at −20 °C for further analysis. All of the proteomic experiments for identification of changes in protein expression between treated and untreated wild-type mc^2155 or *Δmsmeg_3312* strain were performed in biological triplicate.

1.5 Quantitative proteomics analysis and data analysis

For LC-MS/MS analysis, The labeled products were separated using a 60 min gradient elution at a

flow rate of 0.30 μL/min with an UltiMate 3000 RSLCnano System (Thermo Scientific, USA) directly interfaced to a Thermo Q Exactive benchtop mass spectrometer. The analytical column was a custom fused silica capillary tube (75 μm ID, 150 mm length; Upchurch, Oak Harbor, WA, USA) packed with C-18 resin (300 Å, 5 μm, Varian, Lexington, MA, USA). Mobile phase A consisted of 0.1% formic acid, and mobile phase B consisted of 100% acetonitrile and 0.1% formic acid. The Thermo Q Exactive Orbitrap mass spectrometer was operated in data-dependent acquisition mode using Xcalibur 2.1 software. A single full-scan mass spectrum was acquired in the Orbitrap (300–1800 *m/z*, 70000 resolution), followed by 10 data-dependent MS/MS scans at 30% normalized collision energy (HCD) and the dynamic exclusion at 20 S.

The MS/MS spectra from each LC-MS/MS run were searched against the selected database (*M. smegmatis* mc^2155) downloaded from UniProt[22] (download date of December 24, 2014; 6647 entries) using Proteome Discoverer (PD) software, v. 1.4 (Thermo Fisher Scientific, USA). We also added 247 common laboratory contaminants (from the Max Plank Institute of Biochemistry) to our *M. smegmatis* database. The search algorithm SequestHT (in PD software package version 1.4) was used to analyze the data. Standard search parameters were used as follows: One missed cleavage was allowed and fixed post-translational modifications included carbamidomethylation of cysteine residues and TMT sixplexes (K and N-terminal). The oxidation of methionine was set as a variable modification. The precursor ion mass tolerance is set as 10 ppm for all MS data acquired in an Orbitrap mass analyzer. The fragment ion mass tolerance was set at 20 mmu for the MS/MS spectra acquired.

The percolator output provided by PD was used for calculation of the peptide false discovery rate (FDR). The peptide spectrum match (PSM) was considered correct if the *q* value was smaller than 1%. False discovery was determined based on the PSM when searched against a reverse decoy database. The false discovery rate was set to 0.01 for proteins considered unique, and peptides only mapped to a given protein group were considered unique. Relative protein quantification was performed using PD software (Version 1.4) following the manufacturer's instructions for the six reporter ion intensities per peptide. Quantification was performed for proteins with at least two uniquely identified peptides. Quantitative precision is expressed as protein ratio variability. When the protein ratio variability was smaller than 30%, the ratios were accepted as the quantitative ratios of proteins. Differentially expressed proteins were further confirmed by qPCR.

1.6 RNA isolation, RT-PCR and quantitative PCR

Log-phase cultures (OD_{600} of 0.8–1.0) of the tested strains were diluted 1:50 in 7H9 medium. Bacterial cells were harvested by centrifugation when the OD_{600} of the culture reached 0.3. The bacterial pellets were resuspended in TRIzol (Invitrogen, USA), and RNA was purified according to the manufacturer's instructions. cDNA was synthesized using the SuperScript™ III First-Strand Synthesis System (Invitrogen, USA). Quantitative real-time PCR (qRT-PCR) was performed in a Bio-Rad iCycler using 2×SYBR real-time PCR pre-mix (TaKaRa Biotechnology Inc., Japan). Our cycling program follows: 95°C for 90 s, followed by 40 cycles of 95°C for 10 s, 60°C for 10 s, and 72°C for 15 s. DNA-directed RNA polymerase α subunit *rpoD* was selected to normalize gene expression. To evaluate relative gene expression in different strains and/or different treatments, the $2^{-\Delta\Delta Ct}$ method was used[28]. The primers used are listed in.

1.7 Accumulation with semi-automated fluorometric method

To assess fluorochrome GoodView (Fermentas) accumulation, we followed methods previously described with several changes[29]. Briefly,

mycobacteria strains were grown in 7H9 medium, and the cells were collected at an OD_{600} of 0.3. Cultures were collected using centrifugation at 13000 r/min for 10 min, and the pellets were washed in PBS (pH 7.4). The OD_{600} was adjusted to 0.4 with PBS, and glucose was added to a final concentration of 0.4%. GoodView was added at concentrations of 2 mg/L, and the erythromycin was added as indicated. Fluorescence was measured in a microplate reader (Infinite M200 Pro reader, TECAN), using the 491 nm and 530 nm as the excitation and detection wavelengths, respectively. Fluorescence was acquired every 5 min for 30 min at 37 °C. The experiments were repeated three times.

1.8 Measurement of intracellular erythromycin

To analyze the concentration of erythromycin *in vivo* in the wild type strain mc^2155 and knockout strain *Δmsmeg*_3312 with erythromycin treatment, a 50 mL culture of mc^2155 or *Δmsmeg*_3312 was harvested by centrifugation when the OD_{600} of the culture reached 0.3 after erythromycin treatment for 1 h. The cells were washed three times with PBSat (pH 7.2) and resuspended with 70% methanol. Then, extracts were prepared using a Mini BeadBeater (BioSpec) of 5 cycles of 1 min homogenization and 1 min cooling on ice. Lysates were clarified by centrifugation, and erythromycin concentrations were measured using an erythromycin ELISA kit (MLBIO CO., Ltd, Shanghai, China) and calculated following the manufacturer's instruction. This experiment was repeated nine times.

1.9 Statistical analyses

All statistical analyses were performed using the GraphPad Prism 5.0c software. Significant differences in the data were determined by *t*-tests.

2 Results

2.1 MSMEG_3312 is a bacterial hemerythrin-like protein

Recently studies have shown a correlation between redox-related physiological changes and antibiotic treatment[30]. These studies suggest that redox-related proteins influence antibiotic effects. Hemerythrin-like proteins can carry and reversibly bind oxygen[20]; thus, we reasoned that hemerythrin-like proteins might play important roles in maintaining redox balance in mycobacteria and be involved in drug resistance[24]. MSMEG_3312 is involved in drug resistance[26], but the relative mechanisms of MSMEG_3312 resistance to erythromycin have not been explored.

Hemerythrin-like proteins are widely distributed in prokaryotes and invertebrate animals. The characteristic hemerythrin-like protein motif is H…HxxxE…HxxxH…HxxxxD/E[20]. Figure 1 shows the secondary structure of MSMEG_3312. Residues H16, H49, E53, H74, H79, H113 and E118 (numbering based on the MSMEG_3312 sequence) match the typical hemerythrin protein motif. The secondary structure predicted by SWISS-MODEL[31–34] suggested that MSMEG_3312 has a typical hemerythrin-like structure with four α-helices (Figure 1-A).

To confirm the predicted MSMEG_3312 helical structure, we purified MSMEG_3312-His_6 protein from *E. coli*. Circular dichroism (CD) spectra of the *E. coli*-purified MSMEG_3312 show two minima at 208 nm and 222 nm (Figure 1-B). This α-helical protein structure characterization is typical of the CD spectra of previously analyzed bacterial hemerythrins[35]. The UV-visible MSMEG_3312 absorption spectra show peaks at 329 nm and 374 nm, a typical pattern of the di-iron-center of hemerythrin-like proteins[36]. The absorbance peaks disappear after reduction with $Na_2S_2O_4$, which generates the deoxy form by removing oxygen (Figure 1-C). This spectrophotometric analysis indicates that MSMEG_3312 contains the di-iron oxygen bridge typical of hemerythrin-like proteins. Taken together, these bioinformatics, CD, and spectrophotometric results indicate that MSMEG_3312 is a hemerythrin-like protein.

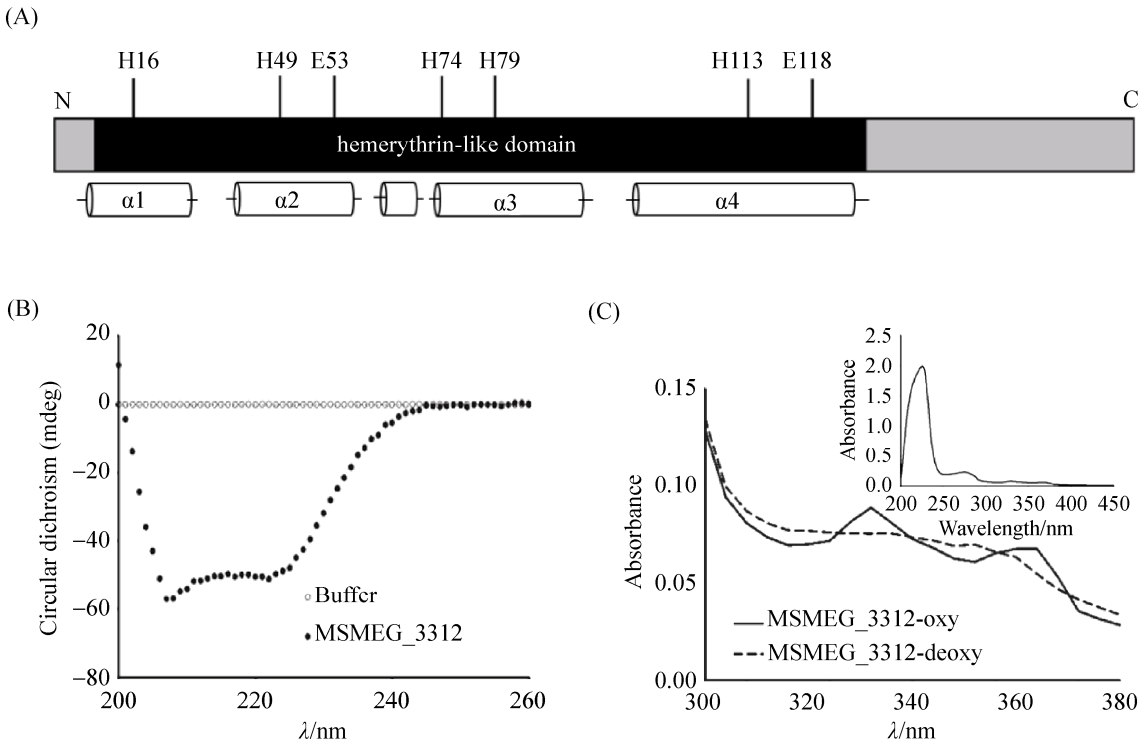

Figure 1. MSMEG_3312 is a hemerythrin-like protein. A: Characteristic hemerythrin-like domain motifs in MSMEG_3312. H represents histidine. E represents glutamate. The lower panel shows MSMEG_3312 secondary structure. The secondary structure prediction was by SWISS-MODEL. B: Circular dichroism spectra of *E. coli*-purified MSMEG_3312. The clear circle indicates the blank control of 20 mmol/L Tris-Cl, pH 7.5 alone. The black circle indicates 100 mg/L MSMEG_3312 protein in 20 mmol/L Tris-Cl, pH 7.5. The measurements were performed at room temperature. Images represent three independent experiments. C: UV-visible absorption spectra of *E. coli*-purified MSMEG_3312. Solid line strands indicate oxidized MSMEG_3312 protein (oxy). Dotted line strands indicate reduced MSMEG_3312 protein (deoxy). Inset indicates the whole spectra for 100 mg/L MSMEG_3312 protein. Images represent three independent experiments.

2.2 Identification of *msmeg_3312*-induced changes in protein expression under normal growth conditions

Using TMT labeling and a mass spectrometric (LC-MS/MS) method, we identified approximately 2800 proteins in each of the samples in three repeated experiments. To explore MSMEG_3312 mechanisms of erythromycin resistance, we compared the protein levels of the wild type mc^2155 strain and mutant strain *Δmsmeg_3312* at the early log phase (OD_{600} of 0.3). Based on the TMT ratios (>1.3 or <0.8) in proteins that have two or more unique peptides, eight up-regulated proteins and 14 down-regulated proteins were identified (Table 1). The false-positive rate was estimated to be less than 1%. To analyze the biological relevance of these proteins, the David Bioinformatics Resource 6.7 Analysis Wizard[37–38] was used to cluster functional annotations. Compared with the *M. smegmatis* genome, the differentially expressed proteins were enriched for metal ion binding (P=2.4×10^{-2}), oxidoreductase activity (P=3.3×10^{-2}), transition metal ion transmembrane transporter activity (P=3.7×10^{-2}), and transition metal ion binding (P=5.8×10^{-2}) functions.

Table 1. Selected proteins that were differentially expressed in mc^{2}155 and *Δmsmeg_3312*

Gene name	Accession	Protein description	Score	Coverage	Peptides matched	Variability/%	Ratio±SD
MSMEG_6638	A0R6Q9	5-methyltetrahydropteroyltriglutamate-homocysteine methyltransferase	56	12	8	4.5–16.0	1.8±0.1
MSMEG_4560	A0R0Z3	ABC Fe3+-siderophores transporter, periplasmic binding protein	85	34	10	6.9–27.0	1.6±0.1
MSMEG_4557	A0R0Z1	ABC transporter, ATP-binding protein	12	20	4	7.6–18.0	1.4±0.1
MSMEG_0530	A0QPV3	Short chain dehydrogenase	14	18	3	0.4–21.0	1.4±0.1
MSMEG_6242	A0R5M3	Alcohol dehydrogenase, iron-containing	50	22	7	0.6–16.9	1.4±0.1
MSMEG_4561	A0R0Z4	ABC Fe3+-siderophores transporter, periplasmic binding protein	38	19	4	5.8–17.7	1.4±0.1
MSMEG_1629	A0QZB3	L-lactate 2-monooxygenase	14	8	3	7.2–19.0	1.3±0.1
MSMEG_3963	A0QSW8	Uncharacterized protein	9	9	3	3.3–23.8	1.6±0.1
MSMEG_6232	A0R5L3	Catalase	20	12	5	6.1–19.1	0.7±0.1
MSMEG_3419	A0QXT5	Uncharacterized protein	25	25	7	1.5–21.5	0.6±0.1
MSMEG_5722	A0R467	Uncharacterized protein	12	69	3	4.7–19.2	0.6±0.1
MSMEG_2115	A0QU83	Uncharacterized protein	14	20	3	0.2–7.3	0.6±0.1
MSMEG_3255	A0QXC8	DoxX	45	24	7	2.8–17.8	0.6±0.1
MSMEG_1131	A0QRI7	Tryptophan-rich sensory protein	26	28	4	0.5–14.8	0.7±0.1
MSMEG_1076	A0QRD4	Uncharacterized protein	45	43	6	0.9–13.2	0.5±0.1
MSMEG_6467	A0R692	DNA protection during starvation protein	40	37	7	4.3–15.8	0.6±0.1
MSMEG_1950	A0QTS8	Uncharacterized protein	120	70	14	3.2–20.7	0.5±0.1
MSMEG_1770	A0QTA4	Uncharacterized protein	102	71	13	7.7–25.6	0.5±0.1
MSMEG_1951	A0QTS9	Conserved domain protein	95	60	17	0.9–9.4	0.5±0.1
MSMEG_6212	A0R5J3	Hemerythrin HHE cation binding domain subfamily protein, putative	11	15	2	9.2–24.3	0.5±0.1
MSMEG_2415	A0QV17	Hemerythrin HHE cation binding region	45	43	9	2.4–18.4	0.4±0.1
MSMEG_6354	A0R5Y1	Serine esterase, cutinase family protein	17	13	2	4.7–16.7	0.3±0.1

The proteomic analysis suggests that, as an oxygen-related protein, MSMEG_3312 influences the protein levels of several reductases and transporters. Two other hemerythrin-like proteins exhibited down-regulation in *Δmsmeg_3312*. Protein levels of A0QV17 (MSMEG_2415) decreased 0.4±0.1 fold in *Δmsmeg_3312* compared with that in mc^{2}155 (Table 1). We also identified seven unique MSMEG_2415 peptides covering 34% of the MSMEG_2415 sequence. The MS/MS spectrum from the proteomic analysis matched the sequence "ELDAQELER" in MSMEG_2415 (Figure 2). qPCR analysis indicates that the mRNA level of *msmeg_2415* decreases by a factor of 0.41±0.05 in *Δmsmeg_3312* compared with that in mc^{2}155 (Figure 3-A). Among the differentially expressed proteins, another predicted hemerythrin-like protein, A0R5J3 (MSMEG_6212), also showed decreased

expression, which was confirmed by qPCR (Table 1 and Figure 3-B). Additionally, two transporters, A0R0Z3 (MSMEG_4560) and A0R0Z4 (MSMEG_4561), were up-regulated and confirmed by qPCR (Table 1 and Figure 3-C, 3-D). Moreover, the mRNA levels of *msmeg_6467* (encoding DPS), and *msmeg_6242* (encoding alcohol dehydrogenase) were down-regulated and up-regulated in *Δmsmeg_3312*, respectively, consistent with changes in the expression of the corresponding proteins A0R692 (MSMEG_6467) and A0R5M3 (MSMEG_6242) (Figure 3-E, 3-F). The fact that so few proteins exhibited changed expression levels might explain the lack of conspicuous growth differences between mc^{2}155 and *Δmsmeg_3312* in 7H9 medium. Furthermore, it suggests that MSMEG_3312 is a stress response protein with no growth effects at normal conditions (i.e. 7H9 medium).

2.3 Expression profiles of mc^{2}155 and *Δmsmeg_3312* in response to erythromycin

The previous comparisons showed no large differences (22 differentially expressed proteins) in protein expression levels between mc^{2}155 and *Δmsmeg_3312*, which is consistent with the observation that both strains grow similarly when cultured in 7H9 medium[26]. We then examined protein expression response when treated with 3.125 mg/L erythromycin in wild-type mc^{2}155 versus Δ*msmeg_3312*. Fewer differentially expressed proteins were identified in mc^{2}155 (proteins were considered to be significantly differentially expressed if the change was >1.3 or <0.8). Upon exposure to 3.125 mg/L erythromycin, only 21 proteins were differentially expressed in wild type mc^{2}155. The differentially expressed proteins detected by MS were assigned using the David Bioinformatics Resource 6.7 Analysis Wizard[37–38]. The 21 proteins are involved in protein disulfide oxidoreductase activity (P=1.3×10^{-2}), response to stress (P=4.8×10^{-2}), and cell redox homeostasis (P=6.3×10^{-2}). Strikingly, a highly induction of A0QTT1 (WhiB7) was observed, with an increase of 2.80±0.74 fold, and the qPCR results show a 98.5±6.5 fold up-regulation with erythromycin treatment, compared with wild type without antibiotic treatment (Figure 3-G).

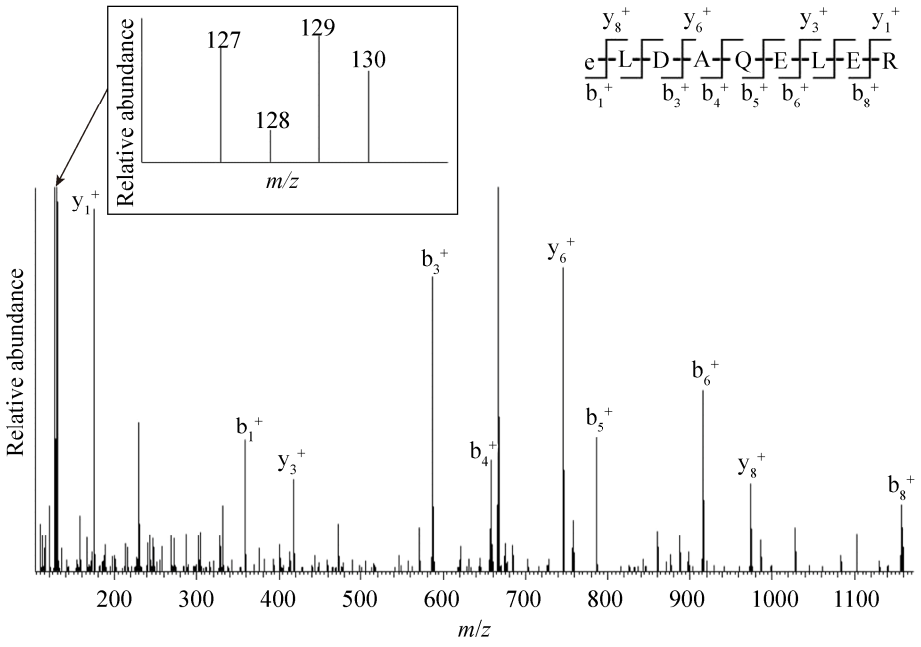

Figure 2. MSMEG_3312 affects the expression of MSMEG_2415 at protein levels. Quantitative comparison of MSMEG_2415 expression using MS/MS.

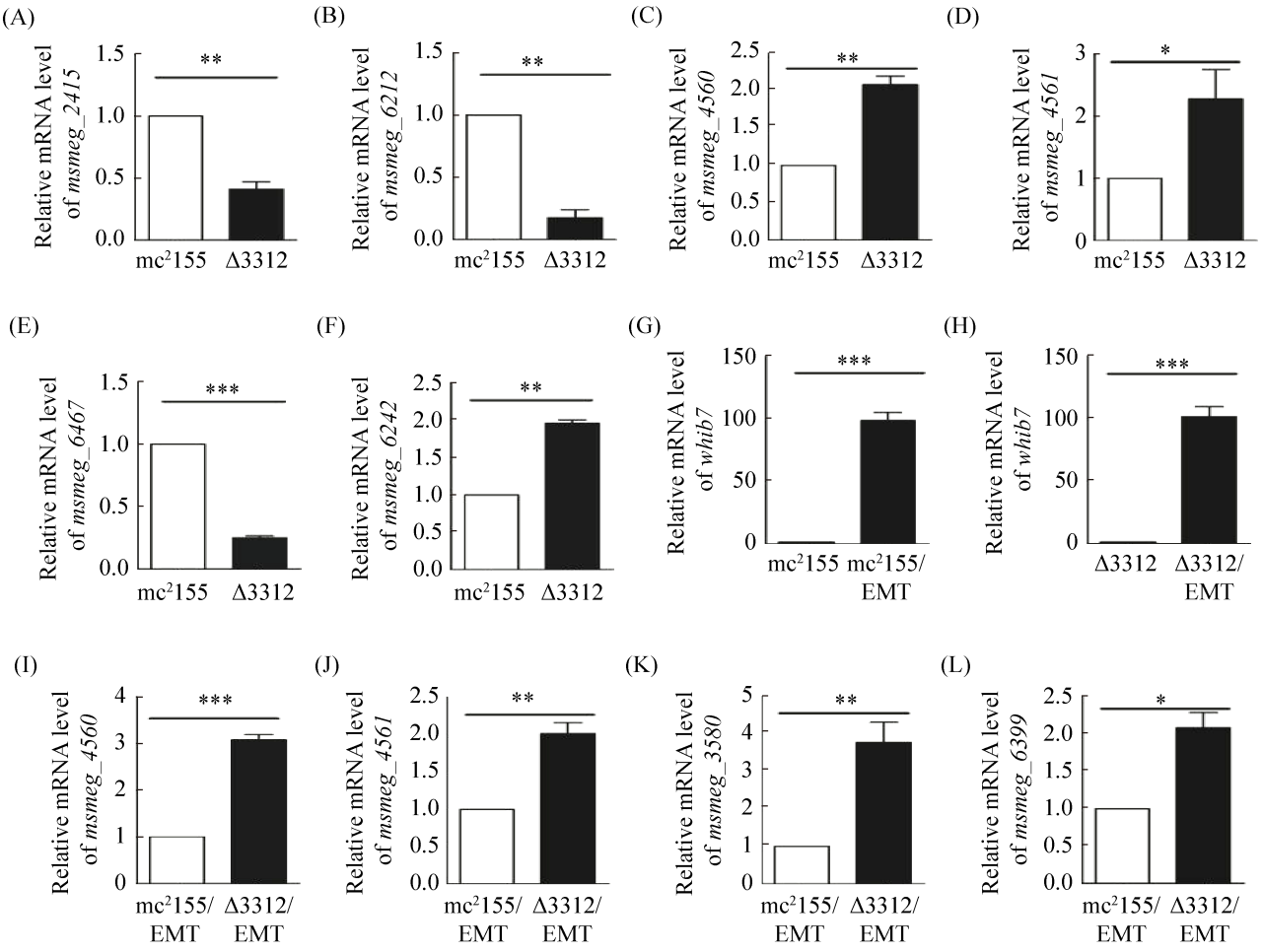

Figure 3. Verification of differentially expressed proteins in mc^{2}155 and *Δmsmeg_3312* with or without erythromycin treatment by q-PCR. A: *msmeg_2415* mRNA levels in mc^{2}155 and *Δmsmeg_3312*. B: *msmeg_6212* mRNA levels in mc^{2}155 and *Δmsmeg_3312*. C: *msmeg_4560* mRNA levels in mc^{2}155 and *Δmsmeg_3312*. D: *msmeg_4561* mRNA levels in mc^{2}155 and *Δmsmeg_3312*. E: *msmeg_6467* mRNA levels in mc^{2}155 and *Δmsmeg_3312*. F: *msmeg_6242* mRNA levels in mc^{2}155 and *Δmsmeg_3312*. G: *whib7* mRNA levels in mc^{2}155 with and without erythromycin treatment (mc^{2}155-EMT). H: *whib7* mRNA levels in *Δmsmeg_3312* with and without erythromycin treatment (*Δ3312*-EMT). I: *msmeg_4560* mRNA levels in mc^{2}155 and *Δmsmeg_3312* after erythromycin treatment (mc^{2}155-EMT and *Δ3312*-EMT). J: *msmeg_4561* mRNA levels in mc^{2}155 and *Δmsmeg_3312* after erythromycin treatment (mc^{2}155-EMT and *Δ3312*-EMT). K: *msmeg_3580* mRNA levels in mc^{2}155 and *Δmsmeg_3312* after erythromycin treatment (mc^{2}155-EMT and *Δ3312*-EMT). L: *msmeg_6399* mRNA levels in mc^{2}155 and *Δmsmeg_3312* after erythromycin treatment (mc^{2}155-EMT and *Δ3312*-EMT).

In contrast, a total of 324 proteins were differentially expressed when *Δmsmeg_3312* was treated with erythromycin. To determine the biological relevance of these proteins, we clustered the differentially expressed proteins based on functional annotation using the DAVID Bioinformatics Resource 6.7 Analysis Wizard[37–38]. Against the whole genome, the differentially expressed proteins assort into 22 categories, including translation (P=4.0×10^{-7}), cellular

homeostasis (P=4.8×10^{-3}), cellular chemical homeostasis (P=1.8×10^{-2}), and others. Similar to the wild type mc^{2}155 strain in response to erythromycin, transcriptional regulator A0QTT1 (WhiB7) was also up-regulated 3.3±0.3-fold at the protein level in *Δmsmeg_3312*, and the qPCR results indicate an increase of 101.6±7.8 fold in response to erythromycin treatment (Figure 3-H). WhiB7 is a Fe-S-dependent transcription factor, and is required for the activation of drug resistance genes. Our results indicate that WhiB7 is an erythromycin induced transcriptional regulator. Moreover, these results suggest that WhiB7 response to erythromycin is independent of MSMEG_3312.

Those differentially expressed proteins between mc^{2}155 and *Δmsmeg_3312* with erythromycin treatment were also compared, and 448 proteins were identified. Twenty-three categories were enriched, including translation (P=7.1×10^{-6}), nitrogen compound biosynthetic process (P=1.0×10^{-5}), homeostatic process (P=5.3×10^{-3}), and others (Figure 4). Among the differentially expressed proteins, the levels of two Ag85C protein, A0QY95 (MSMEG_3580) and A0R624 (MSMEG_6399), were increased 1.9±0.1 fold and 1.4±0.1 fold respectively, in the mutant strain *Δmsmeg_3312*, compared with wild type mc^{2}155 (Table 2). qPCR

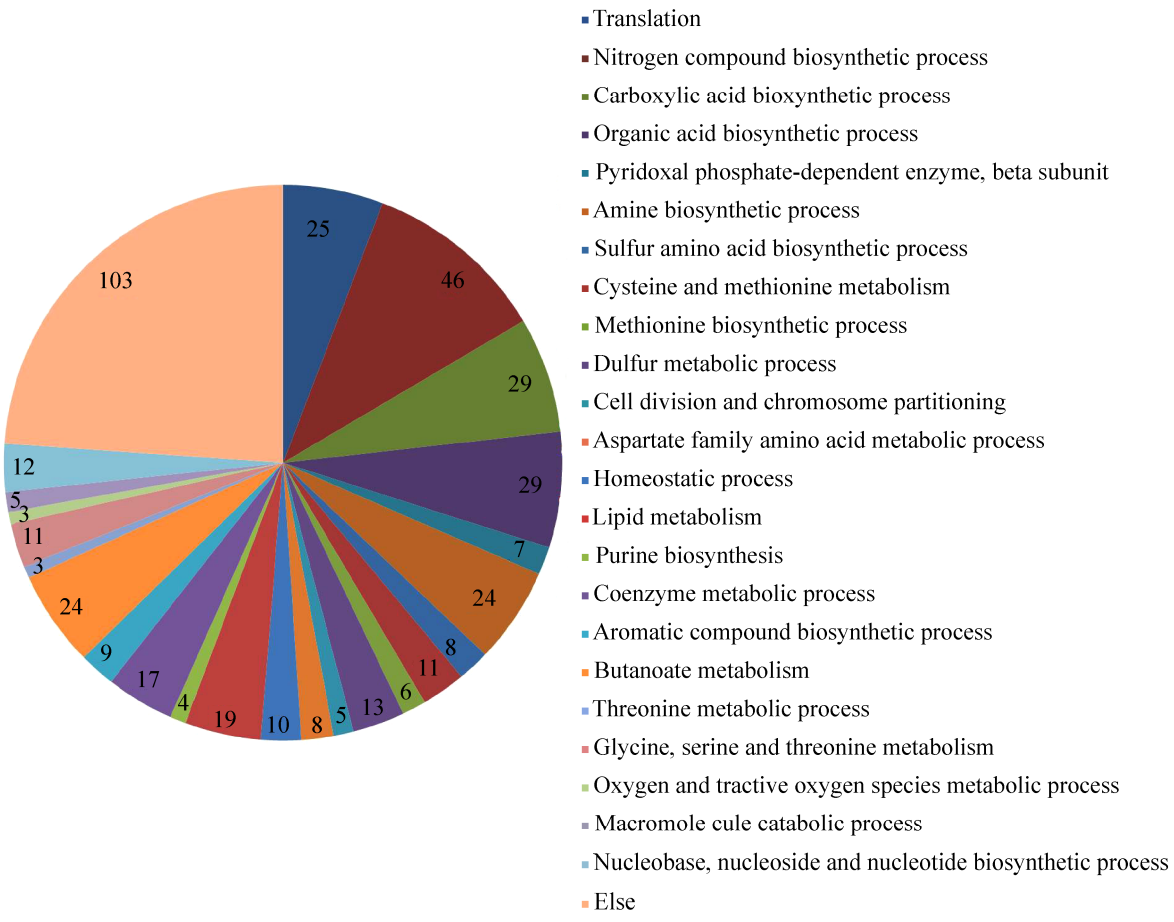

Figure 4. Functional classification of proteins differentially expressed in mc^{2}155 and *Δmsmeg_3312* under erythromycin treatment using the DAVID Analysis Wizard.

Table 2. Selected proteins that were differentially expressed in mc^{2}155 and *Δmsmeg_3312* under erythromycin treatment

Gene name	Accession	Protein description	Score	Coverage	Peptides matched	Variability/%	Ratio±SD
MSMEG_1520	A0QSL4	50S ribosomal protein L36	14	59	3	0.2–7.4	1.9±0.2
MSMEG_3580	A0QY95	Antigen 85-C	24	13	5	4.0–20.2	1.9±0.1
MSMEG_4560	A0R0Z3	ABC Fe3+-siderophores transporter, periplasmic binding protein	62	27	12	2.2–7.4	1.9±0.1
MSMEG_4557	A0R0Z1	ABC transporter, ATP-binding protein	10	13	3	0.9–5.5	1.7±0.1
MSMEG_1437	A0QSD2	50S ribosomal protein L4	98	53	11	9.0–17.6	1.6±0.3
MSMEG_5684	A0R429	Phosphoserine aminotransferase	41	24	11	4.7–12.5	1.6±0.1
MSMEG_3507	A0QY23	Fructose-bisphosphate aldolase	186	75	16	2.8–7.8	1.5±0.2
MSMEG_1473	A0QSG7	50S ribosomal protein L30	27	48	2	9.5–18.8	1.5±0.1
MSMEG_4956	A0R220	Threonine synthase	200	75	20	2.5–12.3	1.4±0.1
MSMEG_6399	A0R624	Antigen 85-C	10	8	2	5.9–7.4	1.4±0.1
MSMEG_4561	A0R0Z4	ABC Fe^{3+}-siderophores transporter, periplasmic binding protein	37	26	5	1.7–9.9	1.4±0.1

analysis indicates that the mRNA levels of *msmeg_3580* (encoding Ag85C) and *msmeg_6399* (encoding Ag85C) were increased by a factor of 3.8±0.5 and 2.1±0.2 respectively, in mutant strain *Δmsmeg_3312* compared with wild type mc^{2}155 with erythromycin treatment (Figure 3-K, 3-L). Ag85C has been shown to have an effect on the cell envelope biogenesis in mycobacteria[39–40] and thus influences cell wall composition. Moreover, 11 transporters were also identified among the differentially expressed proteins. Interestingly, 24 proteins are involved in amino acid synthesis pathways, according to KEGG-User Data Mapping (Figure 4).

2.4 Decreased accumulation of erythromycin in *Δmsmeg_3312*

Quantitative mass spectrometry results showed that the knockout strain *Δmsmeg_3312* exhibits an increased expression of certain transporters both under normal growth conditions and with treatment by erythromycin. We reasoned that an increasing expression of transporters might efflux erythromycin, thus lowering intracellular erythromycin levels compared with mc^{2}155, resulting in better survival. We measured the intracellular erythromycin concentration of both *Δmsmeg_3312* and mc^{2}155 post-treatment with erythromycin for 1 hour: The concentration of intracellular erythromycin in *Δmsmeg_3312* was 19.8±1.9 μg/mL, which was statistically lower than in mc^{2}155 (22.8±1.8 μg/mL) (Figure 5-A). Lower levels of erythromycin were detected in the knockout strain *Δmsmeg_3312* than in mc^{2}155, which might be due to a higher rate of drug export. Furthermore, to rule out the possibility of low drug uptake in the mutant strain, we compared the accumulation of intracellular fluorometric GoodView in both *Δmsmeg_3312* and mc^{2}155. As shown in Figure 5-B, no differences were observed between the mycobacteria strains with or without erythromycin treatment.

3 Discussion

Recent studies have shown that antibiotic treatment

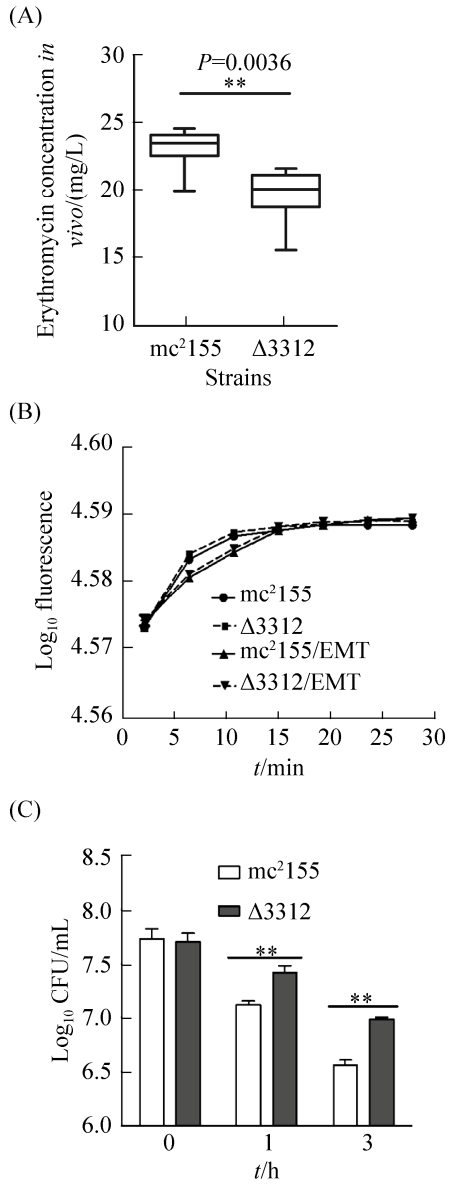

Figure 5. Decreased accumulation of erythromycin in *Δmsmeg_3312* and benefit-growth compared to mc^{2}155. A: Intracellular erythromycin concentration in wild type mc^{2}155 and knockout-strain *Δmsmeg_3312* (Δ3312) under erythromycin treatment. The experiment was repeated for three times. ** P<0.01. B: Accumulation of semi-automated fluorometric curve. Strains were grown in 7H9 medium with the addition of GoodView (2 mg/L) and erythromycin as indicated. The experiment was repeated three times. C: Erythromycin killing curve. Standard deviations are indicated by error bars. *t*-tests were performed using online GraphPad software. The experiment was repeated three times. ** P < 0.01.

influences bacterial protein response and induces bacterial reprogramming in response to these drugs[41]. Antibiotics have complex mechanisms and targets, thus systems biological approaches, such as proteomics, are beginning to allow us to understand the complicated and coordinated system underlying response to drug treatment[42]. In this study, we compared two strains of mycobacteria using quantitative mass spectrometry, one wild-type strain, mc^{2}155, and one *msmeg_3312* knockout strain, *Δmsmeg_3312*, to determine which is more resistant to erythromycin. We observed few differences in protein expression between the strains under baseline growth conditions in 7H9 medium, but 448 proteins were differentially expressed upon treatment with erythromycin. Interestingly, these changes in protein expression included increases in transporters and amino acid synthetic proteins in *Δmsmeg_3312*. Furthermore, our analyses suggest that the knockout strain *Δmsmeg_3312* increases transporter and ribosomal protein expression, and exhibits collective antibiotic tolerance, including antibiotic titration and high population density (Figure 6). To our knowledge, MSMEG_3312 is the first hemerythrin-like protein identified to be involved in antibiotic resistance in mycobacteria.

Erythromycin belongs to the macrolides family; it binds to the 50S subunit of the bacterial ribosomal complex and inhibits protein synthesis[43]. *M. tuberculosis* WhiB7 is a well-identified transcriptional regulator involved in ribosomal-targeting antibiotic resistance, including erythromycin, in mycobacteria[9,44–45]. The characterized erythromycin resistance mechanisms in mycobacteria are complex, including an impermeable mycolic acid-containing cell wall, drug efflux, and antibiotic modification[9,44,46].

Proteomics is a powerful approach for understanding the network of protein changes that respond to drug treatment, facilitating a broad view of antibiotic resistance. This is particularly true when a key gene is found to be involved in drug

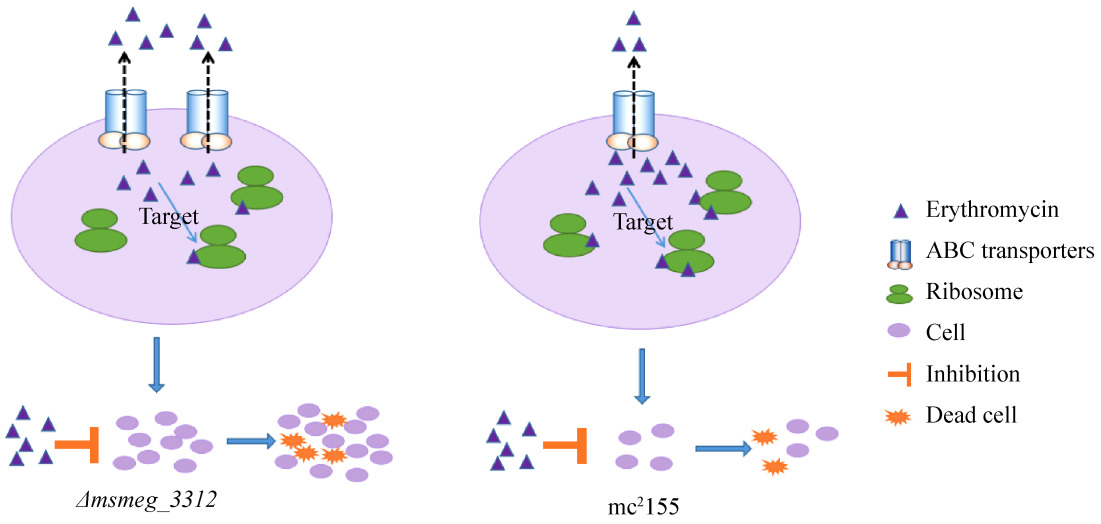

Figure 6. Model of MSMEG_3312 function in erythromycin resistance. More erythromycin was transported out of Δ*msmeg_3312* with high-level expression transporters than from mc^{2}155 during the initial drug treatment.

resistance, which can lead to the development of novel antibacterial therapies[42]. To understand the mechanisms of MSMEG_3312-mediated erythromycin resistance, we compared the differences in mc^{2}155 and *Δmsmeg_3312* protein expression levels using TMT-labeled quantitative proteomics. Consistent with previous studies, WhiB7 (A0QTT1) was highly induced at both protein and mRNA levels in mc^{2}155 (Figure 3-G). WhiB7 was also highly up-regulated in response to erythromycin in *Δmsmeg_3312* (Figure 3-H). The induction of WhiB7 expression in both mc^{2}155 and *Δmsmeg_3312* indicates that the WhiB7-mediated erythromycin resistance pathway is distinct from the MSMEG_3312-mediated erythromycin resistance pathway. Moreover, none of the differentially expressed proteins identified are involved in WhiB7 dependent pathways, such as A0R5B1 (MSMEG_6129), A0R2P5 (TetV) and A0R2G3 (ABC transporter)[47], which suggests that the MSMEG_3312-invovled erythromycin response is via a WhiB7 independent pathway.

Recent studies have shown that efflux pump induction is an important mechanism of drug resistance in many bacteria[46,48–49]. In mycobacteria, the evolution of efflux pumps were an early step in the development of antibiotic resistance[15,50]. Our results show that knocking out *msmeg_3312* increases the protein levels of A0R0Z3 (ABC Fe^{3+} siderophore transporter), A0R0Z1 (ATP-binding ABC transporter), and A0R0Z4 (ABC Fe^{3+} siderophore transporter), compared with the wild type strain mc^{2}155 in the 7H9 medium (Table 1). We reasoned that the transporters with a higher level of constitutive expression, compared with that in wild type mc^{2}155, might show a relative decrease in intracellular erythromycin concentration. Our results show that the concentration of intracellular erythromycin in *Δmsmeg_3312* is significantly lower than in mc^{2}155, as we predicted (Figure 5-A). Moreover, no difference in the accumulation GoodView is found between the mycobacteria strains, which suggests an equal drug uptake in both the resistant strain *Δmsmeg_3312* and wild type mc^{2}155 (Figure 5-B). This also explains why we only observed a low-level of drug resistance in knockout *msmeg_3312* (increment 4×MIC of the wild type strain mc^{2}155)[26]. Based on our results, we provide a model of MSMEG_3312 involvement in erythromycin resistance as part of collective antibiotic tolerance via a combination of diverse

mechanisms, including antibiotic titration and high-density population (Figure 6). More erythromycin is transported out of *Δmsmeg_3312* with high-level expression transporters than from mc^2155 during our initial drug treatments. Furthermore, higher cell survival populations result in relatively lower intracellular concentrations in *Δmsmeg_3312*, than so in mc^2155, and *Δmsmeg_3312* exhibits an advantage over mc^2155 in the presence of erythromycin (Figure 5-C).

We conclude that MSMEG_3312 is a hemerythrin-like protein, and that the *Δmsmeg_3312* strain exhibits increased erythromycin resistance. On the basis of our proteomics results and erythromycin-killing assay, we show that the resistance to erythromycin in strain *Δmsmeg_3312* was not caused by a single event, but by collective antibiotic tolerance, including the transport of erythromycin upon early drug treatment, and a relative concentration decrease via antibiotic titration, followed by the achievement of a high-density population.

参 考 文 献

[1] Brazas MD, Hancock RE. Using microarray gene signatures to elucidate mechanisms of antibiotic action and resistance. *Drug Discovery Today*, 2005, 10(18): 1245–1252.

[2] Dwyer DJ, Kohanski MA, Hayete B, Collins JJ. Gyrase inhibitors induce an oxidative damage cellular death pathway in *Escherichia coli*. *Molecular Systems Biology*, 2007, 3(1): 91.

[3] Kohanski MA, Dwyer DJ, Hayete B, Lawrence CA, Collins JJ. A common mechanism of cellular death induced by bactericidal antibiotics. *Cell*, 2007, 130(5): 797–810.

[4] Eurosurveillance Editorial Team. WHO publishes Global tuberculosis report 2013. *Euro surveillance: bulletin Europeen sur les maladies transmissibles = European communicable disease bulletin*, 2013, 18(43).

[5] Comas I, Coscolla M, Luo T, Borrell S, Holt KE, Kato-Maeda M, Parkhill J, Malla B, Berg S, Thwaites G, Yeboah-Manu D, Bothamley G, Mei J, Wei LH, Bentley S, Harris SR, Niemann S, Diel R, Aseffa A, Gao Q, Young D, Gagneux S. Out-of-Africa migration and Neolithic coexpansion of *Mycobacterium tuberculosis* with modern humans. *Nature Genetics*, 2013, 45(10): 1176–1182.

[6] Bloom BR. Tuberculosis: Pathogenesis, Protection, and Control. Washington, D. C.: ASM Press, 1994.

[7] Zhang HT, Li DF, Zhao LL, Fleming J, Lin N, Wang T, Liu ZY, Li CY, Galwey N, Deng JY, Zhou Y, Zhu YF, Gao YR, Wang T, Wang SH, Huang YF, Wang M, Zhong Q, Zhou L, Chen T, Zhou J, Yang RF, Zhu GF, Hang HY, Zhang J, Li FB, Wan KL, Wang J, Zhang XE, Bi LJ. Genome sequencing of 161 *Mycobacterium tuberculosis* isolates from China identifies genes and intergenic regions associated with drug resistance. *Nature Genetics*, 2013, 45(10): 1255–1260.

[8] Farhat MR, Shapiro BJ, Kieser KJ, Sultana R, Jacobson KR, Victor TC, Warren RM, Streicher EM, Calver A, Sloutsky A, Kaur D, Posey JE, Plikaytis B, Oggioni MR, Gardy JL, Johnston JC, Rodrigues M, Tang PKC, Kato-Maeda M, Borowsky ML, Muddukrishna B, Kreiswirth BN, Kurepina N, Galagan J, Gagneux S, Birren B, Rubin EJ, Lander ES, Sabeti PC, Murray M. Genomic analysis identifies targets of convergent positive selection in drug-resistant *Mycobacterium tuberculosis*. *Nature Genetics*, 2013, 45(10): 1183–1189.

[9] Burian J, Ramón-García S, Howes CG, Thompson CJ. WhiB7, a transcriptional activator that coordinates physiology with intrinsic drug resistance in *Mycobacterium tuberculosis*. *Expert Review of Anti-Infective Therapy*, 2012, 10(9): 1037–1047.

[10] Vilchèze C, Jacobs WR, Jr. The mechanism of isoniazid killing: clarity through the scope of genetics. *Annual Review of Microbiology*, 2007, 61(1): 35–50.

[11] Bardou F, Raynaud C, Ramos C, Laneélle MA, Lanŕelle G. Mechanism of isoniazid uptake in *Mycobacterium tuberculosis*. *Microbiology*, 1998, 144(9): 2539–2544.

[12] Shoeb HA, Bowman BU, Jr, Ottolenghi AC, Merola AJ. Peroxidase-mediated oxidation of isoniazid. *Antimicrobial Agents and Chemotherapy*, 1985, 27(3): 399–403.

[13] Piccaro G, Pietraforte D, Giannoni F, Mustazzolu A, Fattorini L. Rifampin induces hydroxyl radical formation in *Mycobacterium tuberculosis*. *Antimicrobial Agents and Chemotherapy*, 2014, 58(12): 7527–7533.

[14] Koch A, Mizrahi V, Warner DF. The impact of drug resistance

on *Mycobacterium tuberculosis* physiology: what can we learn from rifampicin? *Emerging Microbes & Infections*, 2014, 3(3): e17.

[15] Schmalstieg AM, Srivastava S, Belkaya S, Deshpande D, Meek C, Leff R, van Oers NSC, Gumbo T. The antibiotic resistance arrow of time: efflux pump induction is a general first step in the evolution of mycobacterial drug resistance. *Antimicrobial Agents and Chemotherapy*, 2012, 56(9): 4806–4815.

[16] Hu B, Du J, Zou RY, Yuan YJ. An environment-sensitive synthetic microbial ecosystem. *PLoS One*, 2010, 5(5): e10619.

[17] Udekwu KI, Parrish N, Ankomah P, Baquero F, Levin BR. Functional relationship between bacterial cell density and the efficacy of antibiotics. *Journal of Antimicrobial Chemotherapy*, 2009, 63(4): 745–757.

[18] Hammer BK, Bassler BL. Quorum sensing controls biofilm formation in *Vibrio cholerae*. *Molecular Microbiology*, 2003, 50(1): 101–104.

[19] Bailly X, Vanin S, Chabasse C, Mizuguchi K, Vinogradov SN. A phylogenomic profile of hemerythrins, the nonheme diiron binding respiratory proteins. *BMC Evolutionary Biology*, 2008, 8: 244.

[20] French CE, Bell JML, Ward FB. Diversity and distribution of hemerythrin-like proteins in prokaryotes. *FEMS Microbiology Letters*, 2008, 279(2): 131–145.

[21] Tyagi JS, Sharma D. *Mycobacterium smegmatis* and *tuberculosis*. *Trends in Microbiology*, 2002, 10(2): 68–69.

[22] Hingley-Wilson SM, Sambandamurthy VK, Jacobs WR, Jr. Survival perspectives from the world's most successful pathogen, *Mycobacterium tuberculosis*. *Nature Immunology*, 2003, 4(10): 949–955.

[23] Zahrt TC, Deretic V. Reactive nitrogen and oxygen intermediates and bacterial defenses: unusual adaptations in *Mycobacterium tuberculosis*. *Antioxidants & Redox Signaling*, 2002, 4(1): 141–159.

[24] Li XJ, Tao J, Hu XL, Chan J, Xiao J, Mi KX. A bacterial hemerythrin-like protein MsmHr inhibits the SigF-dependent hydrogen peroxide response in mycobacteria. *Frontiers in Microbiology*, 2014, 5: 800.

[25] Li XJ, Li JJ, Hu XL, Huang LG, Xiao J, Chan J, Mi KX. Differential roles of the hemerythrin-like proteins of *Mycobacterium smegmatis* in hydrogen peroxide and erythromycin susceptibility. *Scientific Reports*, 2015, 5: 16130.

[26] Huang LG, Hu XL, Tao J, Mi KX. A hemerythrin-like protein MSMEG3312 influences erythromycin resistance in mycobacteria. *Acta Microbiologica Sinica*, 2014, 54(11): 1279–1288. (in Chinese)
黄鹂歌, 胡新玲, 陶均, 米凯霞. 耻垢分枝杆菌的蚯蚓血红蛋白样蛋白MSMEG3312影响其大环内酯类药物的敏感性. 微生物学报, 2014, 54(11): 1279–1288.

[27] Hu XL, Li XJ, Huang LG, Chan J, Chen YL, Deng HT, Mi KX. Quantitative proteomics reveals novel insights into isoniazid susceptibility in mycobacteria mediated by a universal stress protein. *Journal of Proteome Research*, 2015, 14(3): 1445–1454.

[28] Livak KJ, Schmittgen TD. Analysis of relative gene expression data using real-time quantitative PCR and the $2^{-\Delta\Delta C_T}$ method. *Methods*, 2001, 25(4): 402–408.

[29] Rodrigues L, Wagner D, Viveiros M, Sampaio D, Couto I, Vavra M, Kern WV, Amaral L. Thioridazine and chlorpromazine inhibition of ethidium bromide efflux in *Mycobacterium avium* and *Mycobacterium smegmatis*. *Journal of Antimicrobial Chemotherapy*, 2008, 61(5): 1076–1082.

[30] Bairoch A, Apweiler R, Wu CH, Barker WC, Boeckmann B, Ferro S, Gasteiger E, Huang HZ, Lopez R, Magrane M, Martin MJ, Natale DA, O'Donovan C, Redaschi N, Yeh LSL. The universal protein resource (UniProt). *Nucleic Acids Research*, 2008, 36(D1): D190–D195.

[31] Arnold K, Bordoli L, Kopp J, Schwede T. The SWISS-MODEL workspace: a web-based environment for protein structure homology modelling. *Bioinformatics*, 2006, 22(2): 195–201.

[32] Guex N, Peitsch MC. SWISS-MODEL and the Swiss-Pdb Viewer: an environment for comparative protein modeling. *Electrophoresis*, 1997, 18(15): 2714–2723.

[33] Kiefer F, Arnold K, Künzli M, Bordoli L, Schwede T. The SWISS-MODEL repository and associated resources. *Nucleic Acids Research*, 2009, 37(D1): D387–D392.

[34] Schwede T, Kopp J, Guex N, Peitsch MC. SWISS-MODEL: An automated protein homology-modeling server. *Nucleic Acids Research*, 2003, 31(13): 3381–3385.

[35] Wirstam M, Lippard SJ, Friesner RA. Reversible dioxygen

binding to hemerythrin. *Journal of the American Chemical Society*, 2003, 125(13): 3980–3987.

[36] Karlsen OA, Ramsevik L, Bruseth LJ, Larsen Ø, Brenner A, Berven FS, Jensen HB, Lillehaug JR. Characterization of a prokaryotic haemerythrin from the methanotrophic bacterium *Methylococcus capsulatus* (Bath). *The FEBS Journal*, 2005, 272(10): 2428–2440.

[37] Huang DW, Sherman BT, Lempicki RA. Systematic and integrative analysis of large gene lists using DAVID bioinformatics resources. *Nature Protocols*, 2009, 4(1): 44–57.

[38] Huang DW, Sherman BT, Lempicki RA. Bioinformatics enrichment tools: paths toward the comprehensive functional analysis of large gene lists. *Nucleic Acids Research*, 2009, 37(1): 1–13.

[39] Jackson M, Raynaud C, Lanéelle MA, Guilhot C, Laurent-Winter C, Ensergueix D, Gicquel B, Daffé M. Inactivation of the antigen 85C gene profoundly affects the mycolate content and alters the permeability of the *Mycobacterium tuberculosis* cell envelope. *Molecular Microbiology*, 1999, 31(5): 1573–1587.

[40] Warrier T, Tropis M, Werngren J, Diehl A, Gengenbacher M, Schlegel B, Schade M, Oschkinat H, Daffe M, Hoffner S, Eddine AN, Kaufmann SHE. Antigen 85C inhibition restricts *Mycobacterium tuberculosis* growth through disruption of cord factor biosynthesis. *Antimicrobial Agents and Chemotherapy*, 2012, 56(4): 1735–1743.

[41] Hancock REW. The complexities of antibiotic action. *Molecular Systems Biology*, 2007, 3(1): 142.

[42] Radhouani H, Pinto L, Poeta P, Igrejas G. After genomics, what proteomics tools could help us understand the antimicrobial resistance of *Escherichia coli*? *Journal of Proteomics*, 2012, 75(10): 2773–2789.

[43] Fair RJ, Tor Y. Antibiotics and bacterial resistance in the 21st century. *Perspectives in Medicinal Chemistry*, 2014, 6: 25–64.

[44] Ramón-García S, Ng C, Jensen PR, Dosanjh M, Burian J, Morris RP, Folcher M, Eltis LD, Grzesiek S, Nguyen L, Thompson CJ. WhiB7, an Fe-S-dependent transcription factor that activates species-specific repertoires of drug resistance determinants in actinobacteria. *Journal of Biological Chemistry*, 2013, 288(48): 34514–34528.

[45] Morris RP, Nguyen L, Gatfield J, Visconti K, Nguyen K, Schnappinger D, Ehrt S, Liu Y, Heifets L, Pieters J, Schoolnik G, Thompson CJ. Ancestral antibiotic resistance in *Mycobacterium tuberculosis*. *Proceedings of the National Academy of Sciences of the United States of America*, 2005, 102(34): 12200–12205.

[46] Del Grosso M, Iannelli F, Messina C, Santagati M, Petrosillo N, Stefani S, Pozzi G, Pantosti A. Macrolide efflux genes *mef*(A) and *mef*(E) are carried by different genetic elements in *Streptococcus pneumoniae*. *Journal of Clinical Microbiology*, 2002, 40(3): 774–778.

[47] Bowman J, Ghosh P. A complex regulatory network controlling intrinsic multidrug resistance in *Mycobacterium smegmatis*. *Molecular Microbiology*, 2014, 91(1): 121–134.

[48] Jumbe NL, Louie A, Miller MH, Liu WG, Deziel MR, Tam VH, Bachhawat R, Drusano GL. Quinolone efflux pumps play a central role in emergence of fluoroquinolone resistance in *Streptococcus pneumoniae*. *Antimicrobial Agents and Chemotherapy*, 2006, 50(1): 310–317.

[49] Louw GE, Warren RM, van Pittius NCG, McEvoy CRE, van Helden PD, Victor TC. A balancing act: efflux/influx in mycobacterial drug resistance. *Antimicrobial Agents and Chemotherapy*, 2009, 53(8): 3181–3189.

[50] Srivastava S, Musuka S, Sherman C, Meek C, Leff R, Gumbo T. Efflux-pump-derived multiple drug resistance to ethambutol monotherapy in *Mycobacterium tuberculosis* and the pharmacokinetics and pharmacodynamics of ethambutol. *The Journal of Infectious Diseases*, 2010, 201(8): 1225–1231.

定量蛋白质组分析蚯蚓血红蛋白样蛋白 MSMEG_3312 介导的分枝杆菌耐红霉素机制

张玉娇[1,2#]，胡新玲[1#]，李晓静[1]，邓海腾[3*]，米凯霞[1,4*]

[1] 中国科学院微生物研究所，中国科学院病原微生物与免疫学重点实验室，北京 100101

[2] 中国科学院大学生命科学学院，北京 101408

[3] 清华大学生命科学学院，北京 100084

[4] 中国科学院大学存济医学院，北京 101408

摘要：【目的】细菌耐药机制是个复杂的机制，系统生物学是系统性揭示耐药机制的有力研究手段。我们课题组前期研究结果显示，蚯蚓血红蛋白样蛋白 *msmeg_3312* 基因敲除后能够增加耻垢分枝杆菌对红霉素的耐药性，本文系统研究 MSMEG_3312 参与红霉素耐药性形成的机制。【方法】首先纯化 MSMEG_3312 蛋白，利用光谱及圆二色谱描述 MSMEG-3312 蛋白。利用定量蛋白质组学的方法比较分析敲除菌株 *Δmsmeg_3312* 与野生型菌株 mc^2155 蛋白表达的差异，并通过 qRT-PCR 进行验证。利用红霉素 ELASA 试剂盒测定 *Δmsmeg_3312* 与 mc^2155 的胞内药物浓度。【结果】光谱及圆二色谱分析确定 MSMEG_3312 是蚯蚓血红蛋白样蛋白。定量蛋白质组学分析发现，红霉素未处理的条件下，相比于野生型菌株 mc^2155，敲除菌株 *Δmsmeg_3312* 有包括 3 种转运蛋白在内的 8 种蛋白表达水平上调，14 种蛋白表达下调；而红霉素处理后，*Δmsmeg_3312* 中有 448 种蛋白差异表达，其中有 11 种转运蛋白表达上调，26 种蛋白与氨基酸合成通路相关。胞内药物浓度检测显示敲除菌株 *Δmsmeg_3312* 的胞内红霉素浓度显著低于野生型菌株。【结论】蚯蚓血红蛋白样蛋白 MSMEG_3312 调控改变了细菌对红霉素药物处理的反应网络，其介导的红霉素耐药是一种集合抗生素耐受机制。

关键词：定量蛋白质组，蚯蚓血红蛋白样蛋白，MSMEG_3312，分枝杆菌，红霉素，耐药性

(本文责编：李磊)

基金项目：国家重点研发计划(2017YFA0505901，2014CB744402)；国家自然科学基金(31670137，31600114，31700128)

[*]**通信作者。**米凯霞，Tel：+86-10-64806082，Fax：+86-10-64807468，E-mail：mik@im.ac.cn；邓海腾，Tel：+86-10-62790498，Fax：+86-10-62797154，E-mail：dengh@biomed.tsinghua.edu.cn

[#]并列第一作者。

收稿日期：2018-01-26；**修回日期：**2018-03-30；**网络出版日期：**2018-05-28